

Epithelial phenotype in total sclerocornea

David Hui-Kang Ma,^{1,2} Lung-Kun Yeh,² Hung-Chi Chen,¹ Anna Marie Chang,³ Yi-Ju Ho,¹ Shirley H.L. Chang,¹ Unique Yang⁴

¹Limbal Stem Cell Laboratory, Department of Ophthalmology, Chang Gung Memorial Hospital, Taoyuan, Taiwan; ²Department of Ophthalmology, Chang-Gung Memorial Hospital, Linko, Chang-Gung University College of Medicine, Taiwan; ³Department of Emergency Medicine, Oregon Health and Science University, Portland, OR; ⁴Department of Biology, University of California, Berkeley, CA

Purpose: To understand whether the epithelial phenotype in total sclerocornea is corneal or conjunctival in origin.

Methods: Four cases of total sclerocornea (male:female = 1:3; mean age = 5.4±4.3; 1–11 years old) who received penetrating keratoplasty (PKP) at our hospital between 2008 and 2011 were included. Corneal buttons obtained during PKP were used for transmission electron microscopy (TEM) as well as immunofluorescence microscopy for cytokeratins 3, 12, and 13, goblet cell mucin MUC5AC, connexin 43, stem cell markers p63 and ABCG2, laminin-5, and fibronectin.

Results: After a mean follow-up period of 38.8±14.0 (12–54) months, the grafts remained clear in half of the patients. TEM examination revealed a markedly attenuated Bowman's layer in the scleralized corneas, with irregular and variably thinned collagen lamellar layers, and disorganization and random distribution of collagen fibrils, which were much larger in diameter compared with a normal cornea. Immunofluorescence microscopy showed that keratin 3 was expressed in all four patients, while p63, ABCG2, and MUC5AC were all absent. Cornea-specific keratin 12 was universally expressed in Patients 1 to 3, while mucosa (including conjunctiva)-specific keratin 13 was negative in these patients. Interestingly, keratin 12 and 13 were expressed in Patient 4 in a mutually exclusive manner. Linear expression of laminin-5 in the basement membrane zone and similar expression of fibronectin were observed.

Conclusions: The epithelia in total sclerocornea are essentially corneal in phenotype, but in the event of massive corneal angiogenesis, invasion by the conjunctival epithelium is possible.

A normal cornea maintains transparency by regular alignment of collagen fibrils as well as the absence of blood vessels (avascularity). Previously, it has been shown that extensive corneal neovascularization (NV) promotes conjunctival epithelial ingrowth (conjunctivalization) into the cornea, mainly through the action of vascular endothelial growth factor (VEGF) [1-3]. However, prior studies mainly focused on chemical burn or autoimmune disease-induced corneal NV, and little is known about whether corneal NV in non-inflammatory or congenital diseases may also promote conjunctivalization. Sclerocornea is a rare form of congenital corneal opacity (CCO) and is characterized by non-inflammatory, non-progressive, and bilateral scleralization of the cornea. Depending upon the extent of involvement, sclerocornea can be further divided into several types, and total sclerocornea is the most severe form [4]. The disease is caused by disordered migration of fetal neural crest cells between the corneal epithelium and the endothelium [5]. Fifty percent of cases of sclerocornea have been reported as either autosomal recessive or dominant, while the remainder are sporadic [6]. Although there is no sex predilection, sclerocornea is

sometimes combined with systemic abnormalities such as mental retardation, deafness, and craniofacial abnormalities [7]. To prevent deprivation amblyopia, penetrating keratoplasty is frequently performed early in childhood [8-11]. However, complications such as allograft rejection or glaucoma are often encountered, which undermine graft survival.

In contrast to the normal avascular cornea, blood vessels are frequently present in scleralized corneas, with vessels from the episclera and the conjunctiva crossing into the cornea [12,13]. Corneal NV not only predisposes the transplanted cornea to allograft rejection but may also facilitate conjunctival epithelial ingrowth [2,3]. To date, it remains unclear whether the surface epithelium of a scleralized cornea is of corneal or conjunctival origin, or a mixture of the two. Since corneal NV is detrimental to graft survival, studying the epithelial phenotype in sclerocornea is important. We used transmission electron microscopy (TEM) and immunofluorescence microscopy to characterize the epithelial phenotype in four specimens of totally scleralized corneas obtained during keratoplasty, and found that the surface epithelia are predominantly corneal in origin, but focal conjunctival invasion may occur in the event of severe corneal NV.

Correspondence to: David Hui-Kang Ma, Chang Gung Memorial Hospital, Taiwan, Phone: (886) 3-3281200 ext. 8652; FAX: (886) 3-3287798; email: davidhkma@yahoo.com

METHODS

This study to examine human corneas with total sclerocornea excised during penetrating keratoplasty (PKP) was approved by the Institutional Review Board of Chang Gung Memorial Hospital, Linko, Taiwan (registry number: 98-2059B). The study was performed adherent to the tenets of the Declaration of Helsinki and the ARVO statement on human subjects. Signed informed consent was obtained from the parents of the patients after the content of the study was explained.

Patients: From 2008 to 2011, four patients with total sclerocornea (male:female = 1:3, mean age = 5.4±4.3; 1–11 years old) received PKP in our hospital. The demographic data of the patients are listed in Table 1. There was no family history of hereditary eye diseases in Patients 1, 3, and 4, but CCO and glaucoma were found in the father and the grandmother of Patient 2. Measured preoperative visual acuity ranged from hand motion (Patient 3) to finger counting at 50 cm (Patient 1). All transplantations were performed under general anesthesia. Donor corneas (6.5 to 7.5 mm in diameter; all 0.5 mm larger than the recipient bed) were punched with a superblade trephine (Pharmacia Production BV, the Netherlands), and the diseased corneas were trephined with the Hessburg-Barron vacuum trephine (Jedmed Instrument, St. Louis, MO). During the operation, the corneas were carefully trephined to avoid cutting through the iris. Extensive iris adhesion to the cornea were noted in Patients 2 and 3, which had to be separated meticulously; while an atrophic iris and lens were seen in Patient 1. The graft was sutured with 16 interrupted sutures of 10–0 nylon suture. Postoperative medications included a topical steroid and antibiotic solution (Tobradex solution, Alcon, Fort Worth, TX), but no systemic prednisolone (5 mg per day) was given except during PKP for the second eye of Patient 4 when the first eye failed due to rejection.

Transmission electron microscopy: Corneal samples from Patients 2 and 3 were fixed in 50 mM phosphate buffer (pH 7.2) containing 2.5% glutaraldehyde and 2% paraformaldehyde for 24 h at room temperature. After refixation in 1% osmium tetroxide for 4 h at room temperature, the corneal samples were washed in PBS (1X; 120 mM NaCl, 20 mM KCl, 10 mM Na₂PO₄, 5 mM K₂PO₄, pH 7.4), dehydrated, and embedded in Epon 812 epoxy resin. The 50 nm ultrathin sections were stained with uranyl acetate and lead citrate, and images were photographed with a Hitachi 7100 transmission electron microscope (Hitachi, Tokyo, Japan) equipped with an AMT Digital camera.

Immunohistochemistry and confocal laser scanning microscopy: Surgically excised scleralized corneas were embedded in optimum cutting temperature (OCT) compound and then were frozen in a –70 °C refrigerator. Immunofluorescent

staining was modified from our previous report [14]. Briefly, 5–7 µm frozen sections were rinsed with PBS and then fixed with 100% methanol at 4 °C for 10 min. Nonspecific reactions were blocked by incubating the sections with PBS containing 2.5% bovine serum albumin (BSA) for 30 min. The slides were then incubated overnight at 4 °C with the appropriate primary antibodies (Table 2), which included antibodies against epithelial differentiation markers keratin 3 and 12 (for the corneal epithelium), keratin 13 (for the conjunctival epithelium), gap junction protein connexin 43 (Cx43), MUC5AC (goblet cell-specific mucin), stem cell markers transcription factor p63 and ATP-binding cassette sub-family G member 2 (ABCG2), laminin-5, and fibronectin. Sections incubated with irrelevant mouse or goat immunoglobulin G (IgG) were used as negative controls. After the sections were washed three times in Tris-buffered saline containing 0.5% Tween-20 for 5 min, they were incubated at room temperature for 1 h with the appropriate secondary antibodies, including cyanine-3 (Cy3)-conjugated donkey anti-mouse IgG (for p63 and ABCG2), fluorescein isothiocyanate (FITC)-conjugated donkey anti-goat IgG (for K12), or FITC-conjugated donkey anti-mouse IgG (for Cx43; keratin 3 and 13; MUC5AC, laminin-5, and fibronectin). Finally, sections were washed three times in Tris-buffered saline with Tween-20 for 5 min and covered with antifade mounting medium containing propidium iodide (PI) or 4',6-diamidino-2-phenylindole (DAPI). Laser confocal microscopy (TCS SP2-MP system; Leica, Heidelberg, Germany) was performed with filters for FITC (excitation 488 nm, emission 500–535 nm), DAPI (excitation 359 nm, emission 450–460 nm), and PI (excitation 514 nm, emission 595–633 nm). The image was averaged from 14 scans within a thickness of 5 to 7 µm. Hematoxylin-eosin (HE) staining was also performed for morphological comparison. Unless particularly mentioned, photos taken in the central region of the specimens are shown.

RESULTS

Surgical outcome: The measured preoperative visual acuity ranged from hand motion (Patient 3) to counting fingers at 50 cm (Patient 1). Postoperatively, elevated intraocular pressure (IOP) was controlled by antiglaucoma agents in all patients. In addition, trabeculectomy was performed in both eyes of Patient 2, but both grafts failed subsequently, and the vision in the oculus dexter (OD) was permanently damaged. After PKP, Patient 3 received lens aspiration and intraocular lens implantation in both eyes. After a mean follow-up period of 38.8±14.0 (12–54) months, grafts remained clear in half of the eyes: Two grafts failed due to glaucoma, one due to allograft rejection, and one to progressive graft edema. For the three

TABLE 1. DEMOGRAPHIC DATA OF PATIENTS.

Patient	Sex	Age	Systemic dx	Eye	Pre-OP VA	Subsequent OP	Final VA	F/U in months	Graft status
1	M	11	Patent ductus arteriosus, ectopic kidney, tethered cord syndrome, hydrocephalus	OD OS	CF/50 CF/20	Lens aspiration (-)	CF/100 20/1000	42 54	Clear Clear
2	F	7	-	OD OS	CF/20 CF/20	Trabeculectomy Trabeculectomy	LS (+) CF/15	51 38	Failed due to poor IOP control Failed due to poor IOP control
3	F	2	-	OD OS	HM HM	Lens asp + IOL Lens asp + IOL	CF/50 20/400	38 49	Mild edema Clear
4	F	1	Mental retardation	OD OS	N/A N/A	N/A N/A	- -	12 26	Clear Failed due to rejection

VA: visual acuity; IOP: intraocular pressure; Lens asp + IOL: lens aspiration + intraocular lens; N/A: not available

TABLE 2. PRIMARY ANTIBODIES, CONCENTRATION, AND THEIR SOURCES.

Antibody	Category	Dilution	Source
Keratin 3	Mouse monoclonal	1:100	Chemicon, now Millipore
Keratin 12	Goat polyclonal	1:50	Santa Cruz Biotechnology, Santa Cruz, CA
Keratin 13	Mouse monoclonal	1:100	Abcam
Keratin 19	Mouse monoclonal	1:50	Abcam
MUC5AC	Mouse monoclonal	1:100	Novocastra, Newcastle-upon-Tyne, UK
Connexin 43	Mouse monoclonal	1:50	Chemicon, now Millipore
P63	Mouse monoclonal	1:50	Chemicon, now Millipore
ABCG2	Mouse monoclonal	1:50	Calbiochem, San Diego, CA
Laminin-5	Mouse monoclonal	1:50	Santa Cruz Biotechnology, Santa Cruz, CA
Fibronectin	Mouse monoclonal	1:50	Sigma-Aldrich

patients who were verbally communicative, vision improved in two (Patients 1 and 3; 20/1,000 and 20/400, respectively) but remained the same (ocular sinister, OS) or worse (OD) in one (Patient 2).

Histology: All four patients presented with diffuse corneal opacity that obscured the iris, and no clear demarcation separated the limbus from the cornea. Palisades of Vogt were identified only in Patient 1 (Figure 1A,E), and various degrees of corneal NV reaching the pupil zone were seen in Patients 2 to 4, most prominently in Patient 4 (Figure 1D,H). Under light microscopy, the stratification of the corneal epithelium and the stromal thickness varied among cases. In general, the epithelia in the central cornea in Patients 1 to 3 resembled the normal corneal epithelium, which contained four to seven layers of superficial squamous and basal cuboidal epithelial cells, but the Bowman's layer was invisible (Figure 1U–X). Increased epithelial stratification from five to 12 layers was noted in the central cornea of Patient 4, and most basal cells were cuboidal or columnar (Figure 1T,X). No goblet cells were seen in any specimen, but with immunohistochemistry, the hyperstratified epithelial cells in Patient 4 were identified as conjunctival (Figure 1X, to the right of the arrow). In Patients 2 to 4, the collagen lamellae in the superficial stroma were more irregularly arranged, while the alignment became more uniform posteriorly (Figure 1Q–T). In Patients 2 and 3, NV was prominent in the anterior corneal stroma (Figure 1R,S; arrowhead), while NV was seen in the entire thickness of the stroma in Patient 4 (Figure 1T; arrowhead). In Patients 2 to 4, stromal hypercellularity was also evident in areas containing corneal NV (Figure 1R–T). Descemet's membrane (DM)-like structure was seen only in Patient 1 (Figure 1Q); in the other three cases, there was no DM, and adhesion of the iris pigment to the posterior stroma was seen in Patients 3 and 4 (Figure 1S,T; arrows). In all four cases, no corneal endothelial cells were seen in the specimens.

Transmission electron microscopy: The ultrastructures of a normal corneal stromal layer consist of regularly arranged collagen fibers along with sparsely distributed interconnected keratocytes (Figure 2A). The collagen fibrils in the stroma are uniformly organized in a lamellar arrangement. Figure 2B,C exhibited the regular arrangement of collagen fibrils in the longitudinal and cross-sectional view, with an average fiber diameter of 35 nm. Figure 2E,I shows the irregular and variably thinned collagen lamellar layers in Patients 2 and 3, respectively. Furthermore, disorganized, nonlinear, and random distribution of collagen fibrils was found in the scleralized stromal tissue (Figure 2F,G,J,K). In contrast to a normal cornea (Figure 2C), the collagen fibers in Patient 3 varied considerably in diameter, ranging from 46 to 78 nm (Figure 2K).

Normal corneal basal epithelial cells with Bowman's membrane are shown in Figure 2D (arrowhead). Note that the anterior stromal collagen is loosely organized. Figure 2H,L shows the irregular and nearly invisible Bowman's membrane in Patients 2 and 3, respectively. In contrast to a normal cornea, collagen fibers in the anterior stroma of Patient 2 are more densely arranged (Figure 2H).

Immunofluorescence microscopy: Using a panel of antibodies against differentiation-related cytokeratins, we showed that immunoreactivity to keratin 3 was homogeneously expressed by the entire layer of the corneal epithelium in Patients 1 and 2, and in the peripheral corneal button in Patient 4 (Figure 3A,B,D). However, signals for keratin 3 were negative in the basal epithelial layer in Patient 3 and the central corneal button in Patient 4 (Figure 3C,D insert). Keratin 12, the acidic cytokeratin pair of keratin 3, and a more specific corneal epithelial marker, was expressed homogeneously in Patients 1 and 2 (Figure 3E,F), but was negative in some basal epithelial cells in Patient 3 (Figure 3G). The immunostaining photos shown in Patients 1 to 3 were from the central cornea,

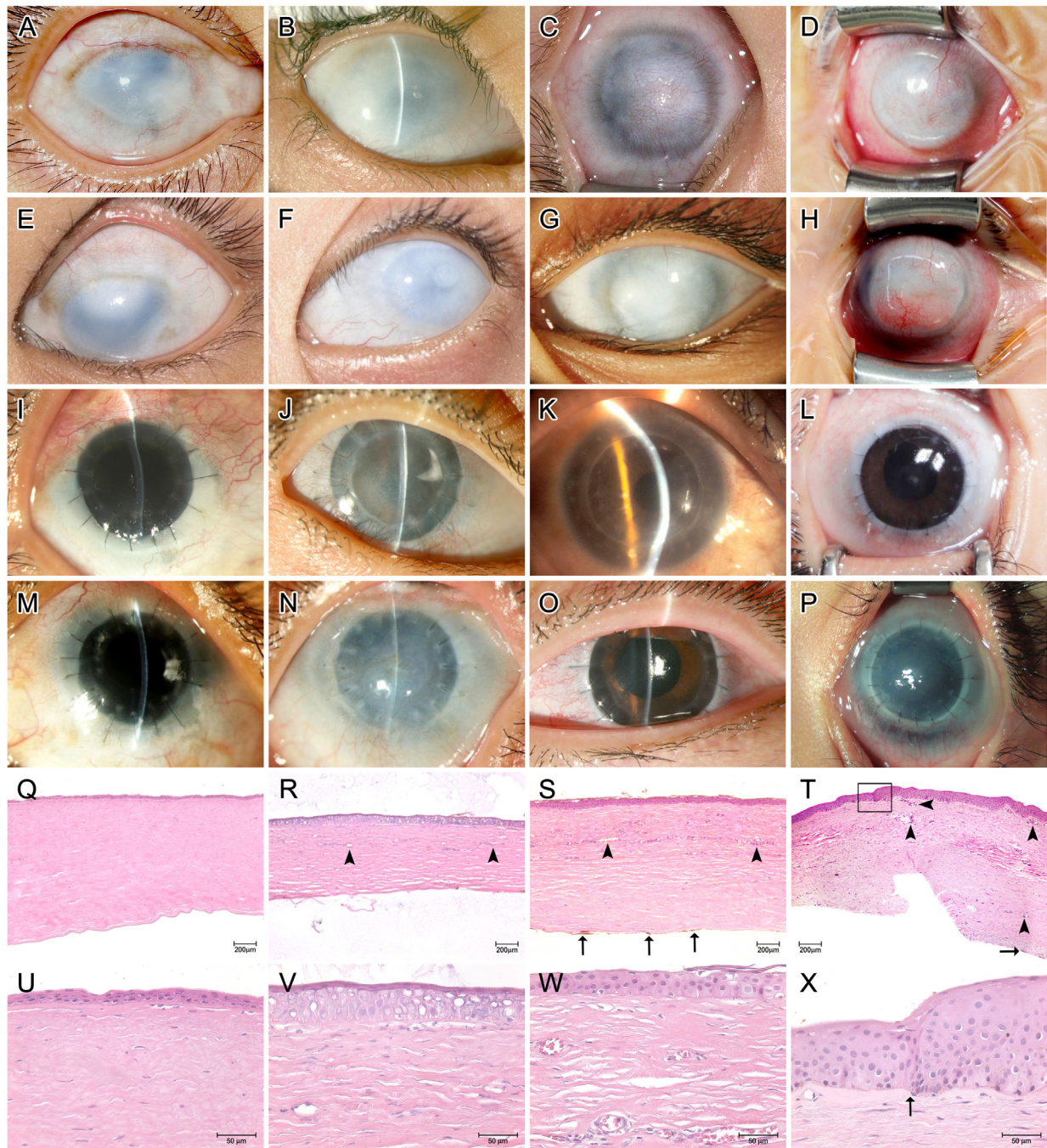


Figure 1. External eye photos and hematoxylin-eosin staining of corneal specimens from four patients with total sclerokernea. **A–H**: Preoperative photos of Patients 1–4. **I–P**: Photos taken at postop 25, 32, 20, and 12 months, respectively. **Q–T**: Hematoxylin-eosin (HE) staining of corneal specimens viewed at 40X. **U–X**: Same specimens viewed at 400X, with emphasis on the corneal epithelium. Note that prominent corneal neovascularization from 5 to 8 O/C is seen in Patient 4 (**H**). Arrowhead: blood vessel in corneal stroma; arrow: iris pigment adhered to posterior corneal stroma; arrow in **X**: junction between corneal (left) and conjunctival epithelium (right) in Patient 4.

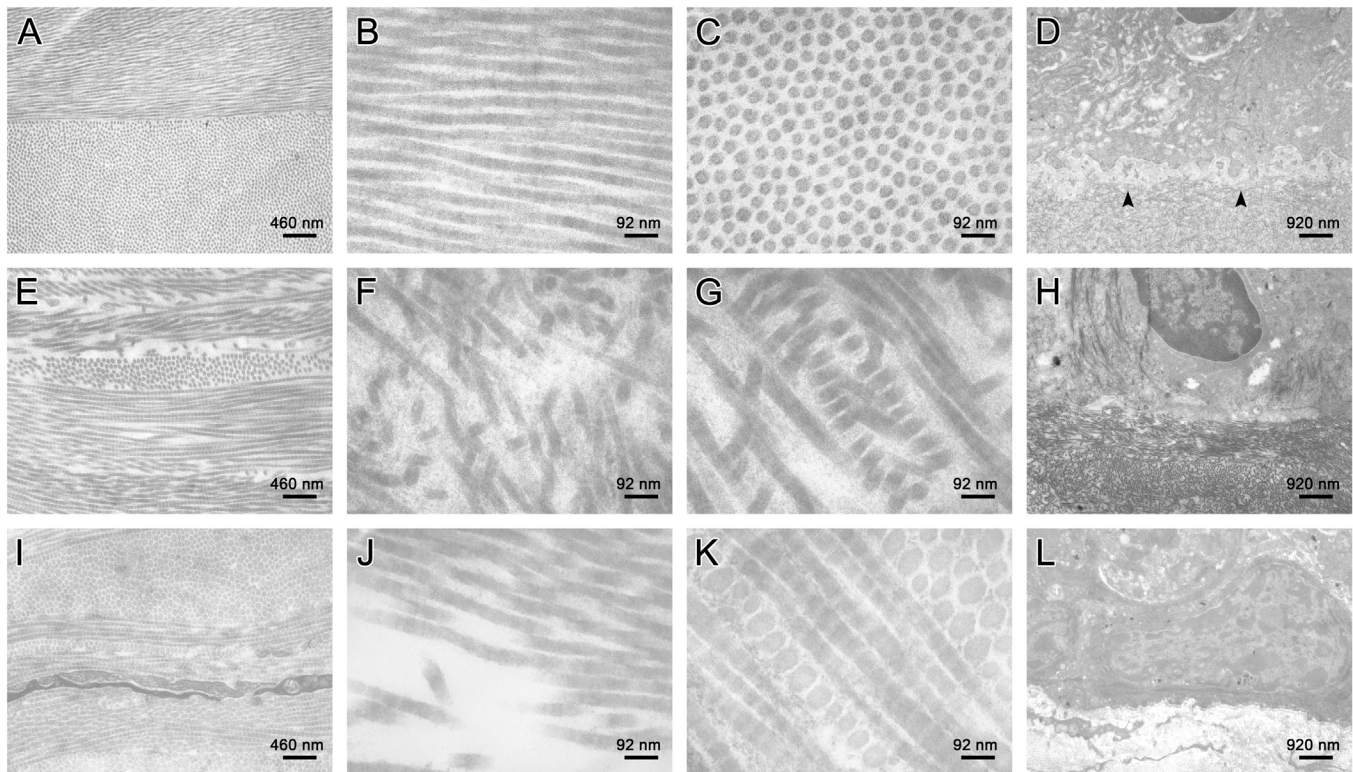


Figure 2. Transmission electron microscopy of normal cornea (A–D) and corneal specimens from Patients 2 (E–H) and 3 (I–L). In the normal cornea, collagen fibrils in the stroma are uniformly organized in a lamellar arrangement (A). Regular arrangement of collagen fibrils in a longitudinal view (B) and a cross-sectional view (C), with an average fiber diameter of 35 nm. Bowman's membrane (arrowhead) is present in the normal cornea (D). Irregular and variably thinned collagen lamellar layers are seen in P 2 (E) and 3 (I), respectively. Disorganized, nonlinear, and random distribution of collagen fibrils in the corneal stroma is also found (F, G, J, and K). The collagen fibers varied considerably in diameter from 46 to 78 nm. In Patients 2 and 3, Bowman's membrane is nearly invisible (H, L). In contrast to the normal cornea in which the anterior stromal collagen is loosely organized (D), the collagen fibers in the anterior stroma of Patient 2 are more densely arranged (H).

and the expression of keratin or other proteins was similar in either the central or peripheral cornea. In Patient 4, however, because of the conjunctival epithelium invasion, different areas were compared, as shown in Figure 3I. In Patient 4, although the peripheral epithelium was keratin 12 positive (Figure 3H, the right peripheral corneal button), keratin 12 was entirely negative in the central cornea except in the focal areas (Figure 3I, insert). In Patient 4, when the specimen was dual-stained with keratin 12 (green) and keratin 13 (red), the peripheral corneal button was keratin 12 positive, while the central cornea was keratin 13 positive, and these two keratins were expressed in a mutually exclusive pattern (Figure 3I). Judging from the keratin expression pattern, this specimen must have contained invading conjunctival epithelium in the center. In Patient 4, the central cornea was covered by the conjunctival epithelium while the peripheral cornea was covered by the corneal epithelium is because the invasion of the conjunctival epithelium was predominantly from the

superior and inferior side, while the corneal button was bisected horizontally (Figure 1T, Figure 3I).

Keratin 13 is expressed by differentiated mucosal epithelia, including conjunctiva and oral mucosa [14,15]. In Patients 1 to 3, staining for keratin 13 was negative (Figure 4A–C); however, in Patient 4, strong suprabasal staining for keratin 13 was evident in the central cornea, while staining at the periphery was negative (Figure 3I, Figure 4D; both photos taken at the right peripheral corneal button). MUC5AC is the mucin secreted by goblet cells. The insert in Figure 4L shows normal conjunctiva containing goblet cells, which were MUC5AC positive. In Patients 1 to 4, the signal for MUC5AC was universally negative, suggesting that none contained goblet cells (Figure 4I–L). Connexin 43 (Cx43) is a gap junction protein often considered a keratinocyte differentiation marker. In Patients 1 to 3, Cx43 staining was present in the entire epithelial layer (Figure 4M–P), similar to the pattern in a normal central cornea. However, Cx43 staining was

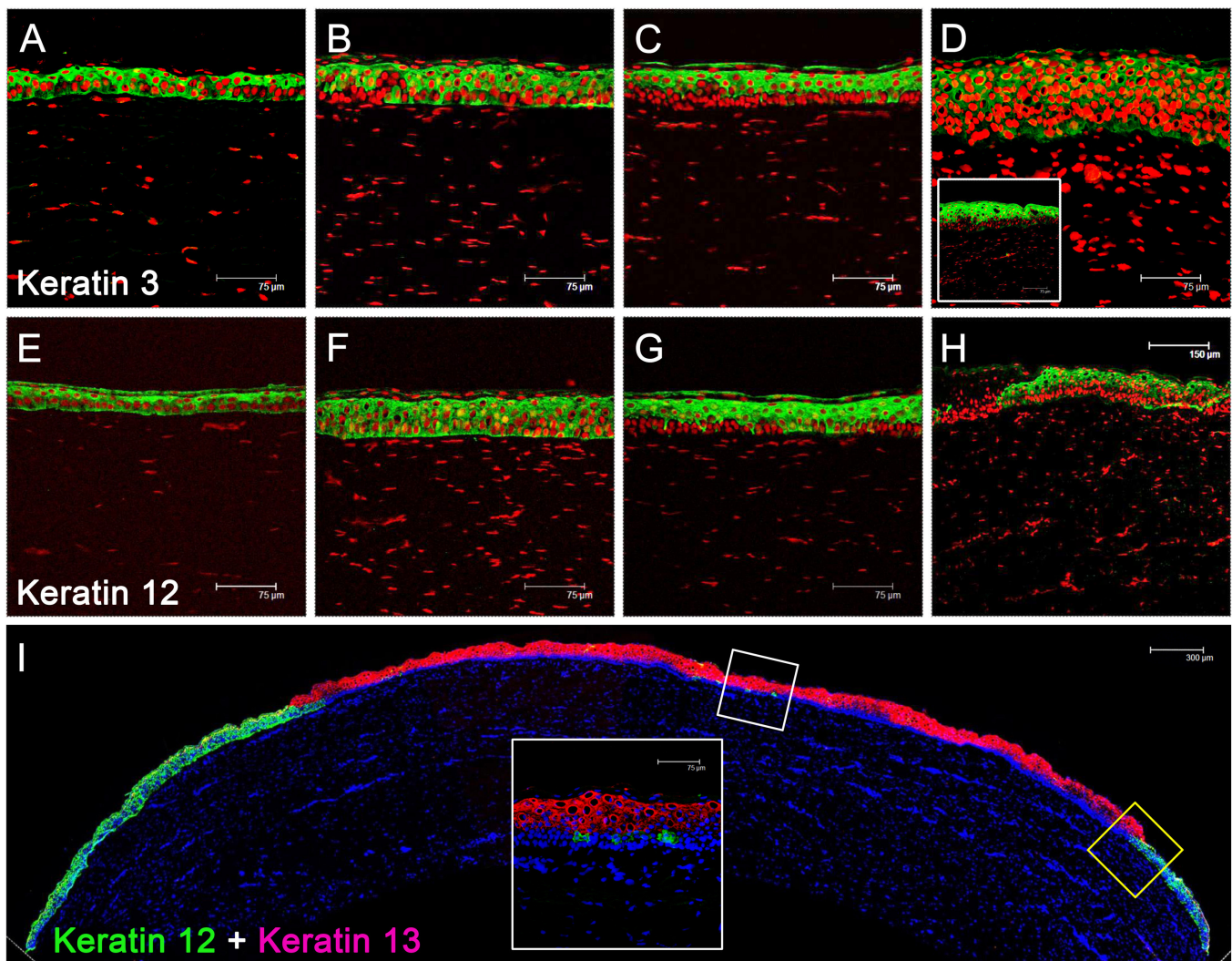


Figure 3. Immunofluorescence microscopy for keratin 3 (A–D) and 12 (E–H) in Patients 1–4, and double staining of keratin 12 (green) and 13 (red) in Patient 4 (I). In all patients, homogenous keratin 3 can be seen; however, the signal for keratin 3 was negative in the basal epithelial layer in Patient 3 (C) and the central cornea of Patient 4 (D insert). Keratin 12 is expressed homogeneously in Patients 1 and 2 (E, F), but is negative in some basal epithelial cells in Patient 3 (G). In Patient 4, keratin 12 is positive in the peripheral cornea (H, I), but entirely negative in the central cornea except in focal areas (I, insert). In Patient 4, the central cornea is keratin 13 positive, suggesting the invasion of the conjunctival epithelium (I). This pattern is due to vertical invasion of the conjunctival epithelium, but the corneal button was bisected horizontally.

predominantly in the superficial and suprabasal epithelial layer but less in the basal epithelial layer in Patient 4 (Figure 4P).

Transcription factor p63, notably the deltaNp63 α isoform, and ATP binding cassette (ABC) transporter ABCG2 have been proposed as markers for corneal epithelial stem cells [16,17]. In all patients, staining for p63 and ABCG2 was invariably negative (Figure 5A–D, E–H), suggesting that the epithelia were more differentiated, similar to the corneal epithelium but not the limbal epithelium. Laminin-5 (LN5; laminin α 3 β 3 γ 2) is a component of the epithelial basement

membrane proteins that facilitate the attachment and migration of basal keratinocytes. In all four specimens, homogenous linear staining of LN5 in the epithelial basement membrane (EBM) zone was evident (Figure 5I–L), suggesting that in these patients the EBM zone was intact. Finally, fibronectin is an extracellular glycoprotein involved in corneal wound healing and epithelial migration. Normally, fibronectin is present in the EBM zone of the corneal, limbal, and conjunctival epithelium [18,19], but during corneal wounding stromal staining of fibronectin can be seen [20]. Linear fibronectin staining was evident along the EBM in Patients 1 to 3, with

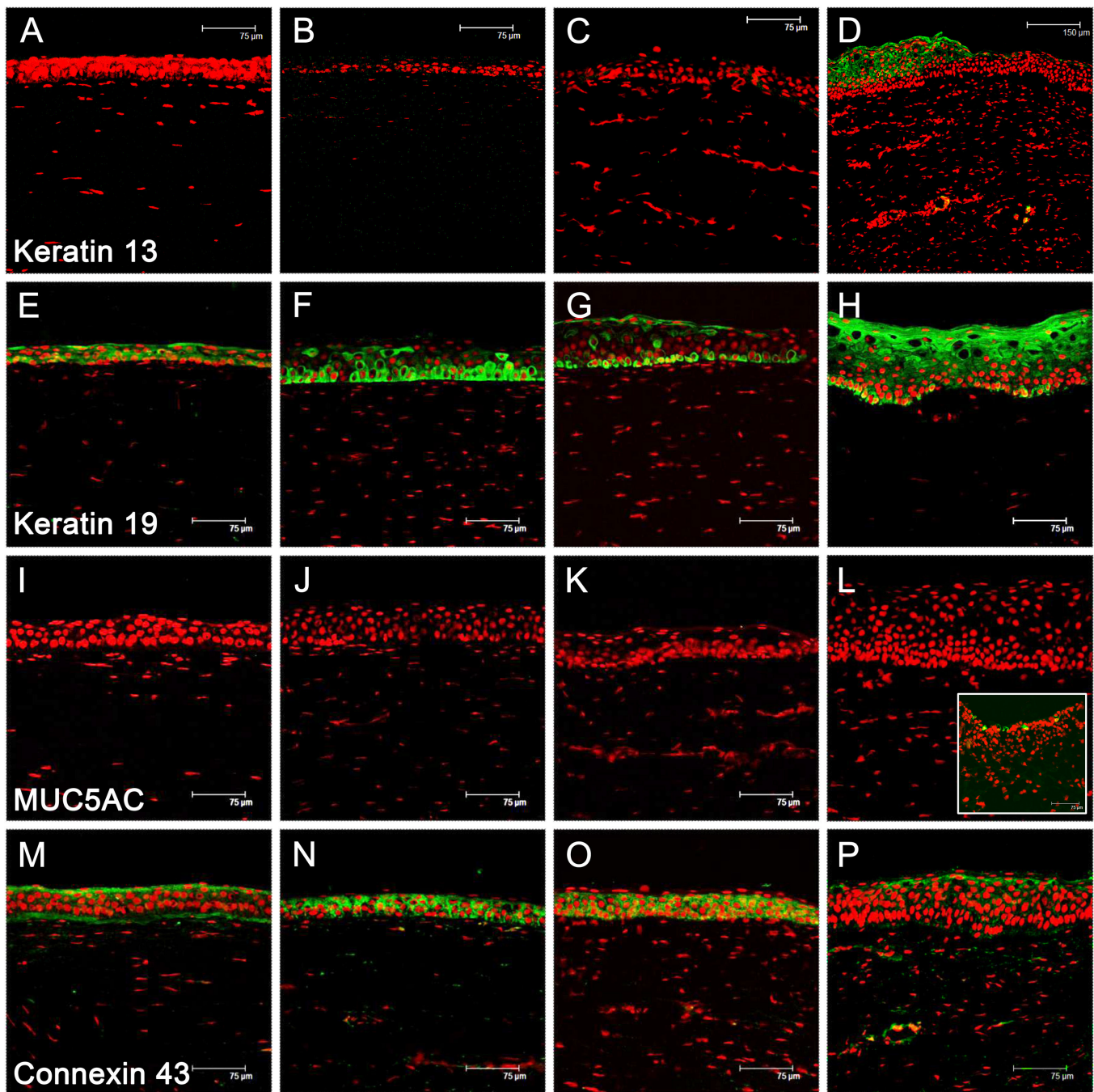


Figure 4. Immunofluorescence microscopy for keratin 13 (A–D), 19, (E–H), MUC5AC (I–L), and connexin 43 (M–P). In patients 1–3, staining for keratin 13 is unanimously negative (A–C); however, in Patient 4, strong suprabasal staining for keratin 13 is evident in the central cornea but not in the peripheral cornea (D). Full-thickness epithelial staining for keratin 19 is seen in Patients 1 and 4 (E, H), and the staining is predominantly in the basal as well as the suprabasal epithelium in Patients 2 and 3 (F, G). In patients 1 to 4, the signal for MUC5AC is universally negative, suggesting that none contains goblet cells (I–L). The insert in 4L shows normal conjunctiva containing goblet cells. In Patients 1 to 3, connexin 43 (Cx43) staining is present in the entire layer of the epithelium (M–O). However, Cx43 staining is predominantly in the superficial and suprabasal epithelial layer in Patient 4 (P).

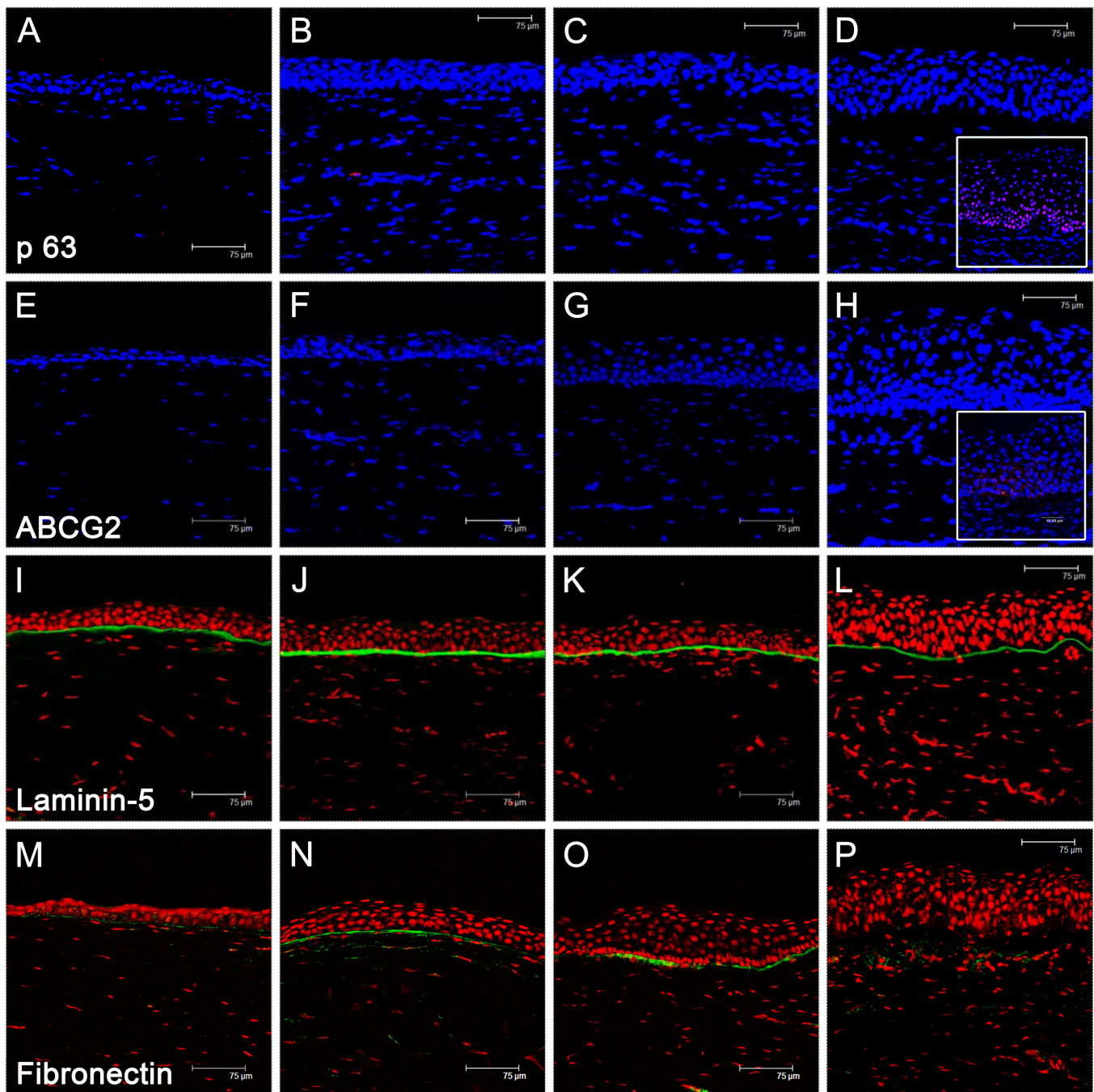


Figure 5. Immunofluorescence microscopy for p63 (A–D), ABCG2 (E–H), laminin-5 (I–L), and fibronectin (M–P). In all patients, staining for p63 and ABCG2 is invariably negative (A–D, E–H; inserts in D and H: positive staining of p63 and ABCG2 in the normal limbus). In all four patients, homogenous, linear staining of laminin-5 in the epithelial basement membrane (EBM) zone is evident (I–L). Finally, linear fibronectin staining is evident along the EBM in Patients 1 to 3, with only sparse staining in the stroma (M–O). Staining of fibronectin in the EBM zone is absent in Patient 4; however, scattered staining is seen in the stroma (P).

only sparse staining in the stroma (Figure 5M-O). Staining of fibronectin in the EBM zone was absent in Patient 4; however, scattered staining was seen in the stroma (Figure 5P).

DISCUSSION

Sclerocornea is a rare form of CCO. Genes implicated in CCO include *paired box 6 (PAX6)*, *pituitary homeobox 2 (PITX2)*, *forkhead box C1 (FOXC1)*, *forkhead box E3 (FOXE3)*, *β 1,3-galactosyltransferase-like (B3GALTL)*, and *keratocan (KERA)*, indicating heterogeneity in a genetic aberration of CCO [21]. For surgical outcomes in infants with CCO, Comer et al. reported overall first graft survival at 12 months was 61%, with ten of 16 eyes retaining a clear corneal graft [10]. Michaeli et al. reported the overall success rate of graft clarity was 78% for congenitally opaque corneas. However, patients with sclerocornea and congenital glaucoma had only a 50% chance of success, with repeated transplants needed for many eyes [9]. In a larger retrospective study, Frueh et al. reported the overall success was 70% in eyes with sclerocornea (27 eyes), 83% for partial sclerocornea (12 eyes), and 100% for Peters' anomaly (17 eyes) after a mean follow-up period of 40 months. Even so, 23 eyes had to be regrafted to maintain corneal clarity [8]. We considered PKP necessary for small children with total sclerocornea so that visual rehabilitation can be undertaken early to alleviate amblyopia. Even if the graft is rejected later, regraft can be arranged to restore corneal clarity in the patient's late childhood or adolescence. Regraft is scheduled for our patients with failed graft but good visual potential. Knowing that the case number reported in this article is small, we did not intend to analyze the surgical result; instead, we focused on investigating the epithelial phenotype in scleralized corneas, which has not been studied before.

Waring et al. classified sclerocornea into four types: isolated peripheral sclerocornea, sclerocornea plana, sclerocornea associated with anterior chamber cleavage anomalies like Peters' anomaly, and total sclerocornea [22]. Histologically, Rezende et al. summarized pathological findings in sclerocornea as follows: 1) The corneal stroma resembles sclera morphologically [23], 2) a precise arrangement of stromal lamellae is absent, 3) the collagen fibers are arranged irregularly, 4) the collagen fiber diameter varies, 5) the thickened collagen fibrils (up to 150 nm in diameter) resembles scleral fibrils, 6) the diameter of the collagen fibrils decreases in the posterior stroma, and 7) Descemet's membrane is attenuated or absent. Among these anomalies, the variation in the diameter of the corneal collagen fibers was the most interesting and characteristic finding [24]. Using TEM, we documented most characteristics of the scleralized corneas

in our specimens. As for the origin of the collagen fibers, previously it was speculated that collagen fibers in scleralized corneas are a direct extension of the sclera; however, Young et al. showed that despite the disorganization of the collagen fibers that resemble those of the sclera, sclerocornea expresses highly sulphated keratan sulfate glycosaminoglycans that resemble those in the cornea, which confirmed the corneal origin of the extracellular matrix in scleralized corneas [25]. Bouhenni et al. reported that the collagen component of the scleralized cornea is similar to that of the normal cornea in that both contain type I but not type III collagen, which is abundant in sclera. Compared with a normal cornea, the keratan sulfate and lumican content in the scleralized cornea is reduced, while that of aggrecan is increased [26].

Total sclerocornea and aniridia are the major two types of anterior segment dysgenesis in which corneal opacity is associated with various degrees of corneal NV. Superficial corneal opacification and vascularization are the two hallmarks in aniridic eyes, caused by *Pax6* mutation and subsequent dysfunction of the limbal stem cell niche, with resulting corneal epithelial stem cell deficiency and conjunctival epithelium invasion [27-29]. To understand whether corneal NV in total sclerocornea may induce conjunctival invasion as in the case of aniridia, we found that the epithelial phenotype in four cases of total sclerocornea was essentially cornea-like; this has not been reported in the literature before. These epithelial cells resemble the normal corneal epithelium in that they are positive for corneal epithelial differentiation markers keratin 3 and 12 and connexin 43, negative for stem cell markers p63 and ABCG2, and negative for goblet cell mucin MUC5AC. However, somewhat different from the corneal epithelium, keratin 3 staining was negative in the basal epithelium in Patients 3 and 4, and in Patient 3, keratin 12 staining was again mostly negative in the basal epithelium. Although our patients were deficient in Bowman's membrane, homogenous staining of laminin-5 suggested the presence of an intact EBM. In a normal cornea, fibronectin appears only in the EBM, but the expression of fibronectin in the stroma increases during corneal wound healing [30-33]. Subepithelial staining for fibronectin notably in Patients 2 and 3 resembles that in the normal cornea, but increased stromal staining as well as cellularity in Patient 4 may imply that the corneal stromal matrix is constantly undergoing remodeling, in which corneal angiogenesis may play a role.

Concomitant with prominent stromal NV, massive conjunctival epithelium invasion was evident in Patient 4. The conjunctival epithelium had increased stratification, positive for keratin 13 but contained no goblet cells. In this case, because the peripheral cornea was covered by the keratin

12-positive corneal epithelium, most likely the cornea still had good epithelial stem cell function; therefore, after PKP the cornea can be covered by the corneal epithelium and remain clear and devoid of blood vessels as shown in Figure 1L. The severity of the conjunctival invasion varied because we had analyzed the epithelial phenotype in the other corneal specimen from Patient 4 and found no conjunctival ingrowth in that cornea (data not shown). Because sclerocornea is heterogeneous in etiology, and we did not perform genetic analysis, the cause of the more prominent corneal neovascularization or conjunctivalization seen in Patient 4 remains unknown. Our findings confirmed the preservation of corneal epithelial cells in the scleralized cornea, so that corneal transplantation can be safely performed without causing corneal epithelial stem cell deficiency and conjunctivalization.

Another interesting finding in Patient 4 was the presence of keratin 12-positive epithelial islands amid the invading conjunctival epithelium (Figure 3I, insert). This phenomenon is similar to Kawasaki et al.'s finding that keratin 12-positive corneal epithelial cells can ectopically reside in the conjunctival epithelium. The researchers found that between 0.2% and 1.7% of the conjunctival epithelial cells collected from the inferior bulbar conjunctiva were keratin 12 positive [34]. Although these keratin 12-positive cells may directly extend from the limbus, they may be maintained by their own stem or progenitor cells in the conjunctiva. However, unlike their report, in our study we did not find any p63 or ABCG2 positive cells near the keratin 12-positive epithelial islands, suggesting that these cells are more mature keratinocytes. Therefore, whether these isolated keratin 12-positive epithelial cells were part of the invading conjunctiva or were the remaining corneal epithelium trapped within the invading conjunctival epithelium remains unknown.

In summary, we analyzed the epithelia in four cases of total sclerocornea, and found the epithelia were essentially corneal in phenotype, yet conjunctival invasion is possible along with massive corneal angiogenesis. These epithelial cells resurfaced the cornea and maintained its integrity after PKP. However, what factor contributes to the differential corneal angiogenesis in scleralized corneas requires further investigation.

ACKNOWLEDGMENTS

The authors thank Ms. Jessica SJ Ma for her technical assistance. The study is supported by the National Science Council grant NMRPG396051 (2010–2013) and Chang Gung Memorial Hospital grant CMRPG3B1101 (2012–2013).

REFERENCES

1. Amano S, Rohan R, Kuroki M, Tolentino M, Adamis AP. Requirement for vascular endothelial growth factor in wound- and inflammation-related corneal neovascularization. *Invest Ophthalmol Vis Sci* 1998; 39:18-22. [PMID: 9430540].
2. Huang AJ, Tseng SC. Corneal epithelial wound healing in the absence of limbal epithelium. *Invest Ophthalmol Vis Sci* 1991; 32:96-105. [PMID: 1702774].
3. Jousseaume AM, Poulaki V, Mitsiades N, Stephen U, Stechschulte, Bernd Kirshhof, Darlene A. Dartt, Guo-Hua Fong, John Rudge, Stanley J. Wiegand, George D. Yancopoulos, Anthony P. Adamis. VEGF-dependent conjunctivalization of the corneal surface. *Invest Ophthalmol Vis Sci* 2003; 44:117-23. [PMID: 12506063].
4. Harissi-Dagher M, Colby K. Anterior segment dysgenesis: Peters anomaly and sclerocornea. *Int Ophthalmol Clin* 2008; 48:35-42. [PMID: 18427259].
5. Elliott JH, Feman SS, O'Day DM, Garber M. Hereditary sclerocornea. *Arch Ophthalmol* 1985; 103:676-9. [PMID: 3994576].
6. Howard RO, Abrahams IW. Sclerocornea. *Am J Ophthalmol* 1971; 71:1254-8. [PMID: 4996988].
7. Idrees F, Vaideanu D, Fraser SG, Sowden JC, Khaw PT. A review of anterior segment dysgeneses. *Surv Ophthalmol* 2006; 51:213-31. [PMID: 16644364].
8. Frueh BE, Brown SI. Transplantation of congenitally opaque corneas. *Br J Ophthalmol* 1997; 81:1064-9. [PMID: 9497466].
9. Michaeli A, Markovich A, Rootman DS. Corneal transplants for the treatment of congenital corneal opacities. *J Pediatr Ophthalmol Strabismus* 2005; 42:34-44. [PMID: 15724897].
10. Comer RM, Daya SM, O'Keefe M. Penetrating keratoplasty in infants. *J AAPOS* 2001; 5:285-90. [PMID: 11641637].
11. Wood TO, Kaufman HE. Penetrating keratoplasty in an infant with sclerocornea. *Am J Ophthalmol* 1970; 70:609-13. [PMID: 4918435].
12. Nischal KK, Naor J, Jay V, MacKeen LD, Rootman DS. Clinicopathological correlation of congenital corneal opacification using ultrasound biomicroscopy. *Br J Ophthalmol* 2002; 86:62-9. [PMID: 11801506].
13. Kanai A, Wood TC, Polack FM, Kaufman HE. The fine structure of sclerocornea. *Invest Ophthalmol* 1971; 10:687-94. [PMID: 4937656].
14. Chen HC, Chen HL, Lai JY, Chen CC, Tsai YJ, Kuo MT, Chu PH, Sun CC, Chen JK, Ma DH. Persistence of transplanted oral mucosal epithelial cells in human cornea. *Invest Ophthalmol Vis Sci* 2009; 50:4660-8. [PMID: 19458337].
15. Ma DH, Kuo MT, Tsai YJ, Chen HC, Hsiao CH, Wang SF, Li L, Lin KK. Transplantation of cultivated oral mucosal epithelial cells for severe corneal burn. *Eye (Lond)* 2009; 23:1442-50. [PMID: 19373264].

16. Di Iorio E, Barbaro V, Ruzza A, Ponzin D, Pellegrini G, De Luca M. Isoforms of DeltaNp63 and the migration of ocular limbal cells in human corneal regeneration. *Proc Natl Acad Sci USA* 2005; 102:9523-8. [PMID: 15983386].
17. de Paiva CS, Chen Z, Corrales RM, Pflugfelder SC, Li DQ. ABCG2 transporter identifies a population of clonogenic human limbal epithelial cells. *Stem Cells* 2005; 23:63-73. [PMID: 15625123].
18. Tervo T, Sulonen J, Valtones S, Vannas A, Virtanen I. Distribution of fibronectin in human and rabbit corneas. *Exp Eye Res* 1986; 42:399-406. [PMID: 3519262].
19. Tuori A, Virtanen I, Aine E, Uusitalo H. The expression of tenascin and fibronectin in keratoconus, scarred and normal human cornea. *Graefes Arch Clin Exp Ophthalmol* 1997; 235:222-9. [PMID: 9143890].
20. Saika S, Kobata S, Hashizume N, Okada Y, Yamanaka O. Epithelial basement membrane in alkali-burned corneas in rats. Immunohistochemical study. *Cornea* 1993; 12:383-90. [PMID: 8306658].
21. Mataftsi A, Islam L, Kelberman D, Sowden JC, Nischal KK. Chromosome abnormalities and the genetics of congenital corneal opacification. *Mol Vis* 2011; 17:1624-40. [PMID: 21738392].
22. Waring GO III, Rodrigues MM. Ultrastructure and successful keratoplasty of sclerocornea in Mietens' syndrome. *Am J Ophthalmol* 1980; 90:469-75. [PMID: 6999882].
23. Rezende RA, Cohen EJ, Uchoa UC, Eagle RC Jr, Wilson RP, Rapuano CJ. Congenital corneal opacities. In: Krachmer JH, Mannis MJ, and Holland EJ, editors. *Cornea*. Elsevier Mosby. 2005:313-38.
24. Ma DH, See LC, Chen JJ. Long-term observation of aqueous flare following penetrating keratoplasty. *Cornea* 2003; 22:413-9. [PMID: 12827045].
25. Young RD, Quantock AJ, Sotozono C, Koizumi N, Kinoshita S. Sulphation patterns of keratan sulphate proteoglycan in sclerocornea resemble cornea rather than sclera. *Br J Ophthalmol* 2006; 90:391-3. [PMID: 16488970].
26. Bouhenni R, Hart M, Al-Jastaneiah S, Alkatan H, Edward DP. Immunohistochemical expression and distribution of proteoglycans and collagens in sclerocornea. *Int Ophthalmol* 2013; 33:691-700. [PMID: 23325424].
27. Nishida K, Kinoshita S, Ohashi Y, Kuwayama Y, Yamamoto S. Ocular surface abnormalities in aniridia. *Am J Ophthalmol* 1995; 120:368-75. [PMID: 7661209].
28. Ramaesh T, Ramaesh K, Martin CJ, Chanas SA, Dhillon B, West JD. Developmental and cellular factors underlying corneal epithelial dysgenesis in the Pax6+/- mouse model of aniridia. *Exp Eye Res* 2005; 81:224-35. [PMID: 16080917].
29. Ramaesh K, Ramaesh T, Dutton GN, Dhillon B. Evolving concepts on the pathogenic mechanisms of aniridia related keratopathy. *Int J Biochem Cell Biol* 2005; 37:547-57. [PMID: 15618012].
30. Maguen E, Rabinowitz YS, Regev L, Saghizadeh M, Sasaki T, Ljubimov AV. Alterations of extracellular matrix components and proteinases in human corneal buttons with INTACS for post-laser in situ keratomileusis keratectasia and keratoconus. *Cornea* 2008; 27:565-73. [PMID: 18520507].
31. Espana EM, Ti SE, Grueterich M, Touhami A, Tseng SC. Corneal stromal changes following reconstruction by ex vivo expanded limbal epithelial cells in rabbits with total limbal stem cell deficiency. *Br J Ophthalmol* 2003; 87:1509-14. [PMID: 14660463].
32. Ishizaki M, Shimoda M, Wakamatsu K, Ogro T, Yamanaka N, Kao CW, Kao WW. Stromal fibroblasts are associated with collagen IV in scar tissues of alkali-burned and lacerated corneas. *Curr Eye Res* 1997; 16:339-48. [PMID: 9134323].
33. Asari A, Morita M, Sekiguchi T, Okamura K, Horie K, Miyauchi S. Hyaluronan, CD44 and fibronectin in rabbit corneal epithelial wound healing. *Jpn J Ophthalmol* 1996; 40:18-25. [PMID: 8739496].
34. Kawasaki S, Tanioka H, Yamasaki K, Yokoi N, Komuro A, Kinoshita S. Clusters of corneal epithelial cells reside ectopically in human conjunctival epithelium. *Invest Ophthalmol Vis Sci* 2006; 47:1359-67. [PMID: 16565369].

Articles are provided courtesy of Emory University and the Zhongshan Ophthalmic Center, Sun Yat-sen University, P.R. China. The print version of this article was created on 11 April 2014. This reflects all typographical corrections and errata to the article through that date. Details of any changes may be found in the online version of the article.